European Conference on Computational Fluid Dynamics
ECCOMAS CFD 2006
P. Wesseling, E. Oñate and J. Périaux (Eds)

STRONG COUPLING OF PARTITIONED FLUID-STRUCTURE INTERACTION PROBLEMS WITH REDUCED ORDER MODELS

Jan A. Vierendeels*

*Ghent University, Dept. of Flow, Heat and Combustion Mechanics
St.-Pietersnieuwstraat 41, 9000 Ghent, Belgium
e-mail: Jan.Vierendeels@UGent.be
web page: http://www.FloHeaCom.UGent.be

Key words: Fluid-Structure Interaction, Partitioned solvers, Reduced order model

Abstract. *The paper describes a new and powerful technique to solve strongly coupled fluid-structure interaction (FSI) problems with partitioned solvers. In order to achieve strong coupling approximate Jacobians of the fluid and structural solvers have to be known. In the proposed method the response to applied displacement and pressure modes are used to build up reduced order models for respectively the fluid and structural solver during the coupling process. The Jacobians of these reduced order models are used to obtain implicit coupling of the reduced order models, finally resulting in an implicit coupling of the partitioned solvers. The method is applied to the flow in the left ventricle during the filling and emptying phase. Two to three modes are needed, depending on the moment in the heart cycle, to reduce the residual by four orders of magnitude and to achieve a fully coupled solution at each time step.*

1 INTRODUCTION

The computation of fluid-structure interaction (FSI) problems has gain a lot of interest in the past decade. The interaction can be loose or strong. For loose coupling problems (e.g. for flutter analysis [1, 2, 3]) existing fluid and structural solvers can be used as partitioned solvers. The main difficulty is the data exchange between those solvers.

When strong interaction is present, strong coupling of the fluid and structural solver can be achieved with a monolithic scheme [4]. However partitioned schemes can also be used for these applications. Vierendeels et al. [5, 6] used a partitioned procedure and reached stabilization of the interaction procedure by introducing artificial compressibility in the subiterations by preconditioning the fluid solver. Recently strongly coupled partitioned methods were developed [7, 8, 9, 10] using approximate or exact Jacobians of the fluid and structural solver. In these methods no black box fluid and/or solid solver can be used.

When existing fluid and structural solvers are used to solve strongly coupled FSI problems, a subiteration process has to be set up for every time step in order to achieve the strong coupling, but in order to obtain convergence typically quite a lot of subiterations are required. Mok et al. [11] used an Aitken-like method to enhance the convergence behaviour of this subiteration process.

In this paper a coupling procedure is presented which outperforms the Aitken-like method for strongly coupled FSI problems. A partitioned procedure is used and implicit coupling is achieved through sensitivity analysis of the important displacement and pressure modes. These modes are detected during the subiteration procedure for each time step. The method allows the use of black box fluid and structural solver. The method is applied to a 2D axisymmetrical model of the cardiac wall which motion is computed during a complete heart cycle. The structural solver was already developed in previous work [5]. As fluid solver the commercial CFD software package Fluent 6.1 (Fluent Inc.) is used to illustrate the practical applicability of the method.

2 METHODS

2.1 Fluid and structural solver

The black box fluid solver which is used has to fulfill some conditions. It must be possible to prescribe the movement of the boundary of the fluid domain through e.g. a user subroutine and it must be possible to extract the stress data at the moving boundaries. In our application we only need the pressure distribution at the moving boundary. The response of the flow solver can be represented by the function F:

$$p_{k+1}^{n+1} = F^{n+1}\left(X_{k+1}^{n+1}\right), \tag{1}$$

where X_{k+1}^{n+1} denotes the prescribed position of the boundary nodes obtained from the structural solver in subiteration $k+1$ when computing the solution on time level $n+1$. It is assumed that the solution on time level n is known. The superscript $n+1$ on F denotes other variables in the flow solver that are already known on time level $n+1$, such as in- and outflow boundary conditions. Starting from time level n the pressure distribution on the boundary nodes p_{k+1}^{n+1} can be computed, which is then passed to the structural solver.

The choice of the boundary conditions needs some attention. When the ventricle is filling the fluid domain has only an inlet, no outlet is present. Therefore it is impossible to specify a velocity at the inlet boundary. This would conflict with the change in volume of the ventricle which is already prescribed by the boundary position on the new time level. Moreover, also the pressure field will be undefined upto a constant value if no pressure boundary is specified. Therefore it is necessary to prescribe the pressure at the inflow boundary during the filling phase and at the outflow during the emptying phase.

The structural model which is used was already developed in previous work [5]. The structural equations are given by G:

$$G^{n+1}\left(X_{k+1}^{n+1}, p_k^{n+1}, \Delta p_{k+1}^{n+1}\right) = 0. \tag{2}$$

Since we are dealing with the cardiac cycle the function G^{n+1} incorporates the prescribed time dependency of the structural properties. In our application, it is assumed that the volume of the ventricle is known as a function of time, therefore the structural solver does not only compute the new position of the boundary nodes, given a pressure distribution at the boundary, but it also computes a pressure shift, Δp_{k+1}^{n+1}, equal for all nodes, so that the volume corresponds with the prescribed volume at that time level. This pressure shift is used to adjust the pressure level in the fluid calculations by adjusting the pressure level of the boundary conditions. In the sequel we denote the structural equations as

$$G^{n+1}\left(X_{k+1}^{n+1}, p_k^{n+1}\right) = 0 \tag{3}$$

for a given pressure input p_k^{n+1} coming from the fluid solver, neglecting the notation for the update of the pressure boundary condition needed in the fluid solver. The structural solver can also be denoted as

$$X_{k+1}^{n+1} = S^{n+1}(p_k^{n+1}). \tag{4}$$

The superscript $n+1$ on F, G and S are dropped from now on. Equation (3) is solved by Newton's method.

2.2 Classical strong coupling methods for partitioned solvers

2.2.1 Explicit subiterations within a time step

Strong coupling can be obtained by calling the fluid and structural solver subsequently during the calculation of a time step until convergence is obtained. When there is a lot of interaction between both subproblems, this approach can lead to divergence in the subiteration process. When underrelaxation is introduced with a constant underrelaxation parameter, divergence can be avoided but convergence is not really obtained as is illustrated below.

A non-constant underrelaxation parameter can be used to improve the convergence of the subiteration process. The underrelaxation parameter can be obtained with an Aitken-like acceleration method [11].

2.2.2 Comparison of the different classical methods

If subsequently the structural solver and the fluid solver are called within the subiterations of a time step, divergence is detected. This is shown in figure 1 for the first time step of the first heart cycle at the onset of filling. Even when underrelaxation is used, convergence within the subiterations could not be obtained in a reasonable number of subiterations (fig. 1). With the Aitken-like method, convergence was also not really obtained for the first time step within a reasonable number of subiterations. During the next time steps even a worse convergence behaviour was observed.

Figure 2 shows the evolution of the position of the boundary during the subiteration process of the first time step when subsequent calls of strucural and fluid solver without underrelaxation are performed. One can detect that the behaviour of low frequency modes are responsable for the divergence behaviour.

From this observation, it can be expected that when implicitness is introduced in the subiteration process for a few low frequency modes, convergence could be obtained.

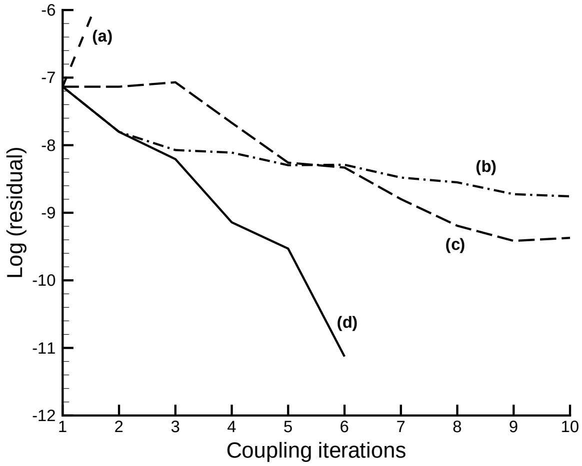

Figure 1: Residual behaviour of the coupling method for the first time step of the first heart cycle at the onset of filling: (a) no reduced order model, without underrelaxation, (b) no reduced order model, with underrelaxation 0.05, (c) no reduced order model, with Aitken-like acceleration technique, (d) with the reduced order models for both the fluid and structural solver.

2.3 Coupling method with a reduced order models for both the fluid and structural solver

In appendex A, it is explained how a reduced order model for the fluid solver can be built up from sets of positions (X_k^f) and corresponding pressure distributions (p_k^f). The superscript $n+1$ is omitted and the superscript f is introduced to distinguish between the fluid and the structural solver. From pressure distributions $(p_{k'}^s)$ applied to the structural solver and the corresponding boundary positions $(X_{k'}^s)$ a reduced order model for the structural solver can be built in the same way as this was done for the fluid solver. The superscript s is used here to denote the structural solver.

After k fluid solver calls and k' structural solver calls the reduced order models, re-

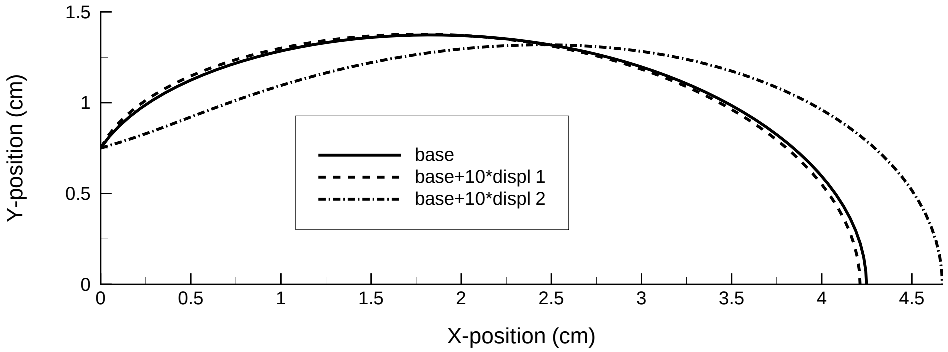

Figure 2: Illustration of the computed displacements of the heart wall if subsequently the structural and fluid solver are called and when no underrelaxation is used.

spectively for the fluid and the structural solver, can be written as:

$$\hat{p}^f_{k+1} = p^f_k + \hat{F}_X\left(X^f_{k+1} - X^f_k\right), \tag{5}$$

$$\hat{X}^s_{k'+1} = X^s_{k'} + \hat{S}_p\left(p^s_{k'+1} - p^s_{k'}\right). \tag{6}$$

A solution for $\left[\hat{p} \;\; \hat{X}\right]^T$ is sought that fulfills both equations, i.e. $\hat{p} = \hat{p}^f_{k+1} = p^s_{k'+1}$ and $\hat{X} = \hat{X}^s_{k'+1} = X^f_{k+1}$. The solution can be found as

$$\begin{bmatrix} \hat{p} \\ \hat{X} \end{bmatrix} = \left(I - \begin{bmatrix} 0 & \hat{F}_X \\ \hat{S}_p & 0 \end{bmatrix}\right)^{-1}\left(\begin{bmatrix} p^f_k \\ X^s_{k'} \end{bmatrix} - \begin{bmatrix} 0 & \hat{F}_X \\ \hat{S}_p & 0 \end{bmatrix}\begin{bmatrix} p^s_{k'} \\ X^f_k \end{bmatrix}\right) \tag{7}$$

This solution can be obtained each time before the fluid or structural solver is called and this solution can then be used as input for these calls. However when calling the fluid solver only the solution for $\hat{X}$ is needed and when the structural solver is called only the solution for $\hat{p}$ has to be obtained. Eqs. (5) and (6) can be solved for $\hat{X}$:

$$\hat{X} = \left(I - \hat{S}_p\hat{F}_X\right)^{-1}\left[X^s_{k'} + \hat{S}_p\left(p^f_k - p^s_{k'} - \hat{F}_X X^f_k\right)\right] \tag{8}$$

or for $\hat{p}$:

$$\hat{p} = \left(I - \hat{F}_X\hat{S}_p\right)^{-1}\left[p^f_k + \hat{F}_X\left(X^s_{k'} - X^f_k - \hat{S}_p p^s_{k'}\right)\right]. \tag{9}$$

The subiteration process to obtain the solution at time level $n+1$ can be summarized as follows. It is obvious that several variants can be constructed based on this idea.

1. Obtain X_1^f with a forward Euler step using position and velocity from the previous time level and compute the corresponding pressure distribution p_1^f with the fluid solver.
2. With $p_1^s = p_1^f$, compute the displacement with the structural solver and obtain X_1^s.
3. Obtain X_2^f by underrelaxing the displacement $X_1^s - X_1^f$ with a factor 0.05 and compute the corresponding pressure distribution p_2^f with the fluid solver.
4. With $p_2^s = p_2^f$, compute the displacement with the structural solver and obtain X_2^s.
5. Build the reduced order model for the fluid solver (5) with 1 mode.
6. Start FSI loop with $k = 2$ and $k' = 2$.
7. Build the reduced order model for the structural solver (6) with $k' - 1$ modes.
8. Compute X_{k+1}^f from the reduced order models with eq. (8).
9. Compute the corresponding pressure distribution p_{k+1}^f with the fluid solver (1).
10. Build the reduced order model for the fluid solver (5) with k modes.
11. Compute $p_{k'+1}^s$ from the reduced order models with eq. (9).
12. Compute the corresponding position of the boundary nodeds $X_{k'+1}^s$ with the structural solver (3).
13. Repeat from step 7 with $k = k + 1$ and $k' = k' + 1$ until convergence is obtained.

3 RESULTS

The method is applied to the filling process of the left ventricle. This FSI problem has already been studied in previous work using the same structural model, but with an own written fluid solver in which artificial compressibility was used as a technique to stabilize and converge the subiteration process [5].

The geometry of the left ventricle is represented by a truncated ellipsoid in the zero stress state. At the zero stress state and with blood at rest, the transmural pressure is zero. The zero stress state is assumed to correspond with a cavity volume of 12 ml, diameter of the mitral annulus of 1.5 cm and base-to-apex distance of 4 cm. These are physiological relevant parameters for a canine heart for which the model was validated.

Away from the zero stress state, the shape of the left ventricle is computed from equilibrium equations for the left ventricular wall. These equilibrium equations involve the time dependent circumferential and longitudinal cardiac stresses, the curvature of the heart wall and the transmural pressure difference. A nonlinear extension of the thin shell equations is used. The position of the mitral valve annulus is kept fixed. We have used Meisner's lumped parameter model for the complete circulation [12] to obtain the necessary boundary conditions for our 2D axisymmetrical calculations. The velocity patterns computed from the Meisner's model at the mitral and aortic valves can be seen in figure 3. From the velocity data, the volume change of the ventricle is computed as a function of time, which is used as input for our calculations as explained above. Since the model is 2D axisymmetrical the position of the mitral valve and the aortic valve is assumed to be the same. This can be done since in normal physiological conditions at most one valve is open at the same time. All details of the model can be found in [5].

Figure 3 shows velocity vectors and pressure contours during the third heart cycle. The time is indicated on the velocity profile diagram which shows the biphasic mitral inflow pattern and the aortic outflow pattern computed with Meisner's model. These results correspond with results which were obtained earlier with another coupling technique presented in previous work [5, 6]. Figure 4 shows the pressure-volume relationship for the three computed heart cycles. It can be seen that convergence for the cycle is already obtained during the second heart cycle. We will further not discuss physiological issues.

Figure 1 shows the convergence behaviour of the proposed method compared to the three explicit coupling procedures during the first time step of the first heart cycle at the onset of filling.

Figure 5 shows convergence results for the proposed method for two different time steps in the third heart cycle (time step 84: slowest convergence and time step 157: fast convergence).

Typically, two to three modes are needed to reduce the residual with three or four orders of magnitude. This is shown in detail in figures 6 and 7 where the number of modes which are used per time step are shown for the third heart cycle.

4 CONCLUSIONS

As conclusion, it can be stated that a very efficient coupling strategy is developed and presented that allows the strong coupling of partitioned solvers. The construction of reduced order models for the black box fluid and structural solvers is crucial to obtain very good convergence. The new approache shows a very good convergence behaviour with respect to the more classical methods.

APPENDIX A

After k subiteration loops (and thus k fluid solver calls) k sets of boundary positions and corresponding pressure distributions are obtained that fulfill the flow equations (1). From the moment that minimum two sets $(X_i, p_i), i = 1 \ldots k$ are available, a set of displacement modes $V_m = \{v_m, m = 1 \ldots k-1\}$ is constructed with

$$v_m = X_k - X_m. \tag{10}$$

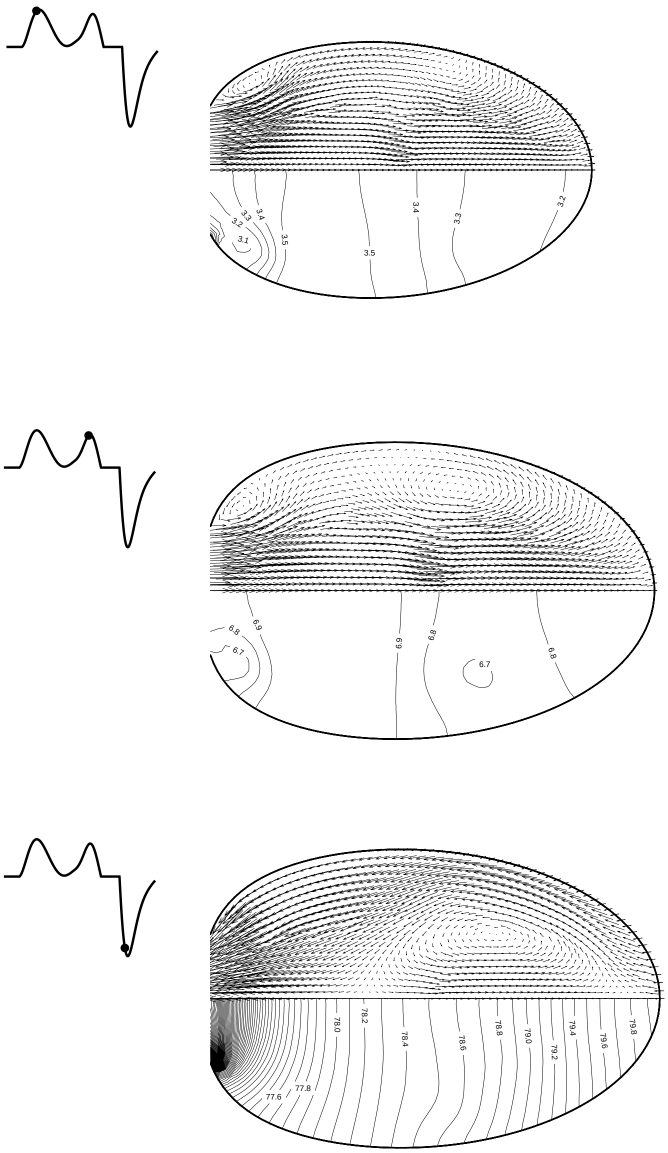

Figure 3: Velocity vectors and pressure contours in the left ventricle during the heart cycle.

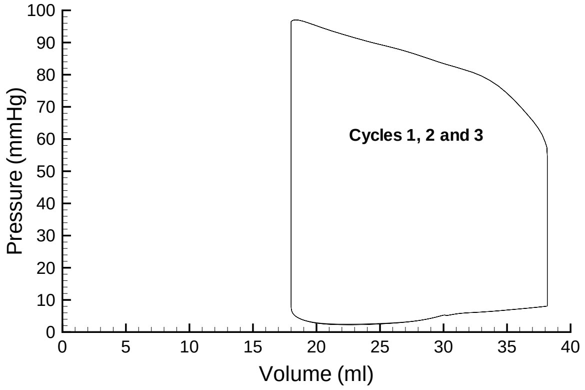

Figure 4: Pressure-volume relationship computed during the first three heart cycles.

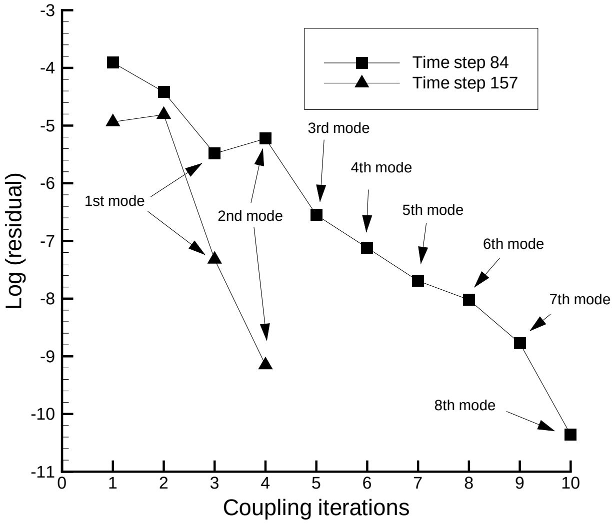

Figure 5: Convergence behaviour of the subiteration process for method 2 for two time steps: time steps 84 and 157 in the third heart cycle.

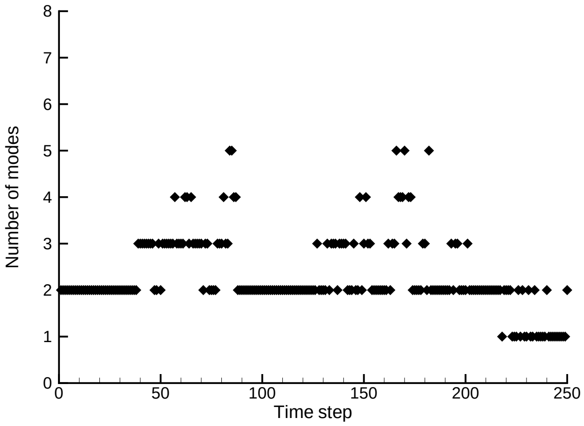

Figure 6: Number of modes needed to reduce the residual below -8 (average of three orders of magnitude) during each time step of the third heart cycle.

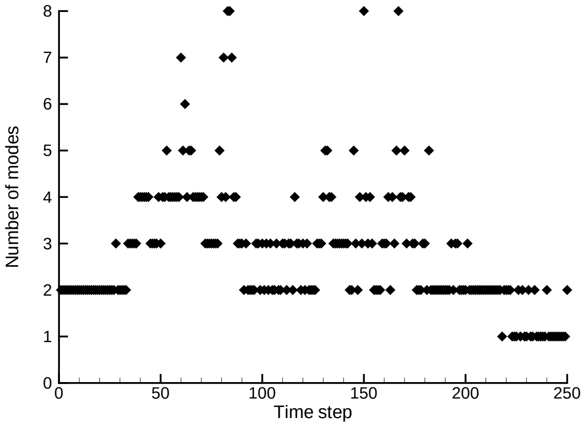

Figure 7: Number of modes used needed to reduce the residual below -9 (average of four orders of magnitude) during each time step of the third heart cycle.

The corresponding pressure mode to v_m is denoted by $\Delta p_m = p_k - p_m$. A pressure mode matrix ΔP_{k-1} is constructed:

$$\Delta P_{k-1} = \left[\begin{array}{ccc} \Delta p_1 & \cdots & \Delta p_{k-1} \end{array} \right], \tag{11}$$

where the columns contain the computed pressure modes.

An arbitrary displacement ΔX can be projected onto the set of displacement modes V_m. The displacement ΔX can be written as

$$\Delta X = \sum_{m=1}^{k-1} \alpha_m v_m + \Delta X_{corr} \tag{12}$$

where α_m denotes the coordinates of ΔX in the set V_m. Note that the number of displacement modes $(k-1)$ is much smaller than the dimension of ΔX, which explains the correction term. If the displacement modes are well chosen, ΔX can be approximated by $\Delta\tilde{X}$:

$$\Delta X \approx \Delta\tilde{X} = \sum_{m=1}^{k-1} \alpha_m v_m. \tag{13}$$

This is an overdetermined problem for the coordinates α_m, which can be faced with the least square approach. With this approach, the coordinates α_m can be computed as

$$\left[\begin{array}{c} \alpha_1 \\ \alpha_2 \\ \vdots \\ \alpha_{k-1} \end{array} \right] = \left[\begin{array}{cccc} \langle v_1, v_1 \rangle & \langle v_1, v_2 \rangle & \cdots & \langle v_1, v_{k-1} \rangle \\ \langle v_2, v_1 \rangle & \langle v_2, v_2 \rangle & \cdots & \langle v_2, v_{k-1} \rangle \\ \vdots & \vdots & & \vdots \\ \langle v_{k-1}, v_1 \rangle & \langle v_{k-1}, v_2 \rangle & \cdots & \langle v_{k-1}, v_{k-1} \rangle \end{array} \right]^{-1} \left[\begin{array}{c} v_1^T \\ v_2^T \\ \vdots \\ v_{k-1}^T \end{array} \right] \Delta X \tag{14}$$

The coordinates α_m denote the amount of each mode in the displacement ΔX so that the corresponding change in pressure Δp can be approximated as

$$\Delta p \approx \Delta P_{k-1} \alpha, \tag{15}$$

where $\alpha = [\alpha_1 \cdots \alpha_{k-1}]^T$. The Jacobian $\hat{F}_X$ of the reduced order model can thus be written as

$$\hat{F}_X = \left[\begin{array}{ccc} \Delta p_1 & \cdots & \Delta p_{k-1} \end{array} \right] \left[\begin{array}{ccc} \langle v_1, v_1 \rangle & \cdots & \langle v_1, v_{k-1} \rangle \\ \vdots & & \vdots \\ \langle v_{k-1}, v_1 \rangle & \cdots & \langle v_{k-1}, v_{k-1} \rangle \end{array} \right]^{-1} \left[\begin{array}{c} v_1^T \\ \vdots \\ v_{k-1}^T \end{array} \right] \tag{16}$$

The reduced order model, used in subiteration $k+1$ is written as

$$\hat{p}_{k+1}^{n+1} = p_k^{n+1} + \hat{F}_X \left(X_{k+1}^{n+1} - X_k^{n+1} \right). \tag{17}$$

REFERENCES

[1] Piperno, S., Farhat, C., Larrouturou, B. Partitioned procedures for the transient solution of coupled aeroelastic problems. I. model problem, theory and two-dimensional application. *Comput. Methods Appl. Mech. Engrg.*, **124**, 79–112, (1995).

[2] Farhat, C., Lesoinne, M., Le Tallec, P. Load and motion transfer algorithms for fluid/structure interaction problems with non-matching discrete interfaces: momentum and energy conservation, optimal discretization and application to aeroelasticity. *Comput. Methods Appl. Mech. Engrg.*, **157**, 95–114, (1998).

[3] Geuzaine, P., Brown, G., Harris, C., Farhat, C. Aeroelastic dynamic analysis of a full f-16 configuration for various flight conditions. *AIAA J.*, **41**, 363–371, (2003).

[4] Hübner, B., Walhorn, E., Dinkler, D. A monolithic approach to fluid-structure interaction using space-time finite elements. *Comput. Methods Appl. Mech. Engrg.*, **193**, 2069–2086, (2004).

[5] Vierendeels, J.A., Riemslagh, K., Dick, E., Verdonck, P.R. Computer simulation of intraventricular flow and pressure gradients during diastole. *J. Biomech. Eng.-T. ASME*, **122**, 667–674, (2000).

[6] Vierendeels, J.A., Dick E., Verdonck, P.R. Hydrodynamics of color m-mode doppler flow wave propagation velocity v(p): a computer study. *J. Am. Soc. Echocardiog.*, **15**, 219–224, (2002).

[7] Gerbeau, J.-F., Vidrascu, M. A quasi-newton algorithm based on a reduced model for fluid structure problems in blood flow. *Mathematical Modelling and Numerical Analysis (M^2AN)*, **37**, 631–647, (2003).

[8] Matthies, H.G., Steindorf, J. Partitioned strong coupling algorithms for fluid-structure interaction. *Comput. Struct.*, **81**, 805–812, (2003).

[9] Heil, M. An efficient solver for the fully coupled solution of large-displacement fluid-structure interaction problems. *Comput. Methods Appl. Mech. Engrg.*, **193**, 1–23, (2004).

[10] Fernández, M.A., Moubachir, M. A newton method using exact jacobians for solving fluid-structure coupling. *Comput. Struct.*, **83**, 127–142, (2005).

[11] Mok, D. P., Wall, W. A., Ramm, E. Accelerated iterative substructuring schemes for instationary fluid-structure interaction. *Computational Fluid and Solid Mechanics (K. Bathe, ed.)*, Elsevier, (2001) 1325–1328.

[12] Meisner, J. *Left atrial role in left ventricular filling: dog and computer studies*, Phd dissertation, Albert Einstein College of Medicine, Yeshiva University, New York, U.S.A., (1986).